

Weighted Quasi Interpolant Spline Approximation of 3D point clouds via local refinement

Andrea Raffo^{1,2} and Silvia Biasotti³

¹*Department of Applied Mathematics and Cybernetics, SINTEF, Oslo, Norway.*

²*Department of Mathematics, University of Oslo, Oslo, Norway.*

³*Istituto di Matematica Applicata e Tecnologie Informatiche “E. Magenes” CNR, Genova, Italy.*

Abstract

We present a new surface approximation, the *Weighted Quasi Interpolant Spline Approximation* (w-QISA), to approximate very large and noisy point clouds. We adopt local implicit representations based on three key ingredients: 1) a local mesh for the piecewise implicit representation $z = f(x, y)$ that defines where the approximation will be more detailed, 2) a weight function for the approximation of the control points that captures the local behavior of the point cloud, and 3) a criterion for global (or local) refinement. The present contribution addresses the theoretical properties of the method, focusing on global and local bounds, shape preservation, local shape control and robustness. The accuracy of this representation is tested against real data from different types of surfaces.

Keywords: spline models, local refinement, LR B-splines, surface reconstruction, approximation methods, point clouds.

1 Introduction

The ever-growing availability of 3D data acquired by laser scanners, photogrammetry and diagnostic devices and the easing of creating virtual objects and scenes has been inducing an exponential growth of the data available and the need of efficient data representations. A good representation model must be, at the same time, *efficient*, that is based on the minimum amount of data, yet *effective*, that is, able to support conservative conclusions and keep as much information as possible. To handle large 3D data volumes it is often necessary to adopt approximation strategies so that a single point becomes a representative of a region or a set of properties [AG15].

An efficient approximation and representation allows to recover the digital representation of a physical shape that commonly contains a variety of properties and defects, such as geometric features, noise or outliers and so on. For instance, when the acquisition conditions are not optimal (low resolution of instruments, motions, etc.) or different acquisition techniques collect data sets of different resolution or the data are incomplete (e.g, in the digitalization and reconstruction of broken artifacts or scans of objects partially occluded [Geo17]).

This work addresses the surface reconstruction problem with quasi-interpolant polynomial surfaces from raw point sets. The method exhibits a number of theoretical properties (e.g., global and local bounds, local refinement, adaptivity to boundary conditions) as well as a number of desirable practical ones such as robustness to variable noise, outliers and computational efficiency.

1.1 Contributions

Our method is specifically designed to approximate huge amounts of low quality points. The main advantages in our technique can be summarized as follows.

- *Piecewise polynomial surfaces.* We approximate 3D point clouds via a piecewise-algebraic quasi-interpolant. The evaluation of spline spaces is computationally more convenient, with respect to the common radial basis functions, as (piecewise) polynomial bases require low-order integration scheme to be correctly computed. The use of piecewise algebraic approximations makes our method suitable also to CAD applications, where B-splines and NURBS are *de facto* the standard tools. Moreover, the treatment of essential boundary conditions is more natural than in meshless methods, as it relies on the number of repetition of each knot value.
- *Local representation.* Splines' property of local support make them highly parallelizable, speeding approximation and evaluation up.
- *Global and local bounds.* Local and global bounds are provided, as they give a theoretical basis on the quality of the resultant approximation.
- *Special configurations.* Meshes for spline representations can be easily modified, with the purpose of changing the continuity between elements or interpolating data.
- *Shape preservation.* The method has a general definition, that allows to change the weight function or adapt it to the input point set. This permits, in general, to preserve shape information such as monotonicity and convexity.
- *Robustness and reduced computational cost.* Weight functions act as noise and outliers filters in the computation of the control points, making it possible to model highly perturbed point clouds. Compared to the traditional approaches, the computational complexity is considerably reduced given that the method stands basically on weighted averages.
- *Local shape control.* An additional key strength, which distinguishes our technique from traditional pure implicit ones, is the local shape control. This allows to easily represent complex shapes and to quickly increase the precision in those regions where more detail is required.

1.2 Organization

The remainder of the paper is organized as follows. Section 2 overviews the existing surface reconstruction techniques focusing on methods based on implicit and parametric surfaces. In Section 3 we introduce some basic definitions and results about uni- and bi-variate spline spaces. In Section 4, the core of our paper, we present the general idea behind the new spline based approximation method Section 4.2 details how it is possible to locally refine the model and provides an outline of the main algorithm. Section 5 presents several application examples. Discussions and concluding remarks are provided in Section 6.

2 Previous Work

Existing surface reconstruction methods can be broadly categorized into two main representation schemes: polygonal meshes and surface-based models. The literature in this field is vast and we cannot do justice to it here. We limit here to reference surface-based

models relevant to our approach; for a survey on surface reconstruction methods we refer to [BTS⁺14].

An important class of implicit surfaces is based on Blinn's idea of blending local implicit primitives, called *blobs* [Bli82]. Pratt [Pra87] discusses the possibility to fit scattered data with algebraic surfaces, where the so-called algebraic distance is combined with a linear normalization of the coefficients. Muraki [Mur91] integrates the above two ideas by using a linear combination of Gaussian blobs to fit the point cloud. Function Representations (FRep) [PASS95], that allow to express implicit representations in terms of elementary objects (primitives), have been applied to model microstructures [PVFA10].

Signed distance functions compute, for each point, the signed distance to the nearest point of the surface are a widely adopted for surface reconstruction, because the ideal surface can be seen as the zero set of such a distance function. Taubin [Tau91] formulates the reconstruction problem in terms of the minimization of a quadratic loss function, whose solution is found by solving a generalized eigenvalue problem. Hoppe et. al [HDD⁺92] use a reconstruction algorithm that locally approximate the signed distance function via a local tangent plane construction. Lim et al. [LTGS95] introduce a technique for a blended union of spherical primitives. Bajaj et al. [BBX95] and Bernardini et. al [BBCS99] use low-degree patches, where the coefficients hold certain sign constraints to guarantee the desired topology structure. Curless and Levoy [CL96] propose a volumetric approach to shape reconstruction based on a cumulative weighted signed distance function. Kazhdan et. al [KBH06] show a Poisson surface reconstruction technique, consisting of the approximation of the indicator function of the underlying surface. Mullen et al. [MGDCS10] considers global stochastic signing of distance functions. The method of [FC11] incorporates positional, gradient and Hessian constraints, where the Hessian has been proved to improve the modeling of those regions with missing data [KH13]. In [LA13], shape primitives are used to resample the point cloud and enforce sharp feature constraints in the output. Levin [Lev03] uses projection moving least squares (PMLS) to reconstruct a smooth surface from a point cloud (i.e. a point-set surface). This idea is then used by Alexa et al. [ABCO⁺01] in point-based graphics. Amenta and Kil [AK04] formally define a point-set surface as the set of local minima of an energy function. Shen et al. [SOS04] devise an implicit MLS (IMLS), in order to interpolate (or approximate) implicit surfaces from polygonal data. Fleishman et al. [FCOS05] propose the robust MLS fitting technique, which can simultaneously process noise and sharp features. Feng et al. [FYD14] devise the model multiple curves/surfaces approximation, that allow to separate mixed scanning points received from a thin-wall object and consist of a second-order extension of the PMLS. The signed or unsigned distance function and MLS surface approximations may have a limited usage due to the absence of an analytical expression. Savchenko et al. [SPOK95], Carr et al. [CBC⁺01], Dihn et al. [DST01] and Turk and O'Brien [TO02] use globally supported radial basis functions (RBFs) interpolant for smooth surface reconstruction. Morse et al. [MYR⁺01] and Kojekine et al. [KHS03] employ compactly supported RBFs to handle large datasets.

Ohtake et al. [OBA⁺03] first introduce the multilevel partition of unity (MPU) with three different types of local approximation to recover sharp features. Later, the MPU construction got combined with compactly-supported radial basis functions [OBS05]. Nagai et al. [NOS09] defines differential operators directly on the MPU function.

Sedeborg [Sed85] firstly introduced piecewise algebraic surfaces within a tetrahedral lattice of control points. Lee et al. [LWS97] use a quasi-interpolant, the Multilevel B-spline Approximation (MBA), where the coefficients depends on values of tensor product B-splines defined on lattices. Jüttler and Felis [JF02] use tensor product B-splines to have some desirable properties from both global and local approximations. Rouhani and Sappa [RS11] extend the 3L algorithm to implicit tensor product B-spline spaces and

later developed a reconstruction algorithm based on the partition of unity technique [RSB15]. Dokken [Dok96] firstly defined approximate implicitization of parametric (hyper)surfaces in CAD, that later was numerically implemented by Barrowclough [BD12] and applied to patches approximation for CAD reverse engineering in [RBM18]. Shalaby et al. [STW⁺06] numerically compare Jüttler’s and Dokken’s technique to compute an approximate implicit representation of point clouds sampled from existing surfaces. Skytt et al. [SBD15] apply least square fitting and MBA of locally refined spline surfaces to terrain data. A comparison between RBFs and LR B-splines approximations has been performed by Patané et al. [PCS⁺17].

As general observations, on one hand, implicitly defined functions offer representations that reduce geometric queries such as inside/outside to mere function evaluations; are usually more resistant to noise and work well with non-uniformly distributed point clouds. However, approaches based on implicit surface fitting produce interpolation matrices that may become ill-conditioned, resulting in a numerical instability that negatively affects the computation of an accurate solution. Approximation techniques for surface implicitization can considerably reduce the instability but, no matter which technique is used, the storage requirement for implicit representations is relatively large. On the other hand, parametric representations allow to simply generate points on the modeled surface, which is why they got predominant in most CAD systems. Our approach belongs to both these two families of methods and permits an adaptive refinement in correspondence of model details, keeping a good robustness to noise and outliers.

3 Basic concepts

We briefly remember some basics on uni- and bivariate spline spaces, as we will use them for the formulation of our local approximation. We then outline some of the current approaches to local refinement.

3.1 Univariate B-splines

Let $n \in \mathbb{N} \setminus \{0\}$ and $p \in \mathbb{N}$. From B-splines theory, it is well known that a non-decreasing sequence $\mathbf{x} = [x_1, \dots, x_{n+p+1}]$, which is commonly referred to as *global knot vector*, generates n B-splines of degree p over \mathbf{x} . In practice, the construction of each of such B-splines requires only a subsequence of $p+2$ knots, collected in a *local knot vector*.

Definition 3.1 (Univariate B-spline). Let $\mathbf{x} := [x_1, \dots, x_{p+2}]$ be a (local) knot vector. A B-spline $B[\mathbf{x}] : \mathbb{R} \rightarrow \mathbb{R}$ of degree p is the function recursively defined by

$$B[\mathbf{x}](x) := \frac{x - x_1}{x_{p+1} - x_1} B[\mathbf{x}^1](x) + \frac{x_{p+2} - x}{x_{p+2} - x_2} B[\mathbf{x}^2](x), \quad (1)$$

where $\mathbf{x}^1 := [x_1, \dots, x_{p+1}]$, $\mathbf{x}^2 := [x_2, \dots, x_{p+2}]$ and

$$B[x_i, x_{i+1}](x) := \begin{cases} 1, & \text{if } x \in [x_i, x_{i+1}) \\ 0, & \text{elsewhere} \end{cases}, \quad i = 1, \dots, p+1.$$

Here, the convention is assumed that “ $0/0 = 0$ ”.

By assuming $x_1 < x_{p+2}$, it follows that $B[\mathbf{x}]$ is a piecewise polynomial of degree p . The continuity at each unique knot is $p-m$, where m is the number of times the knot is repeated. $B[\mathbf{x}]$ is smooth in each open subinterval (x_i, x_{i+1}) , where $i = 1, \dots, p+1$, and is non-negative over \mathbb{R} . The support of $B[\mathbf{x}]$ is the compact interval $[x_1, x_{p+2}]$.

Definition 3.2 (Univariate spline space). Given a global knot vector $\mathbf{x} = [x_1, \dots, x_{n+p+1}]$, the spline space $\mathbb{S}_{p,\mathbf{x}}$ is the linear space defined by

$$\mathbb{S}_{p,\mathbf{x}} := \text{span} \{B[\mathbf{x}_1], \dots, B[\mathbf{x}_n]\},$$

where $\mathbf{x}_i := [x_i, \dots, x_{i+p+1}]$ for any $i = 1, \dots, n$. An element $f \in \mathbb{S}_{p,\mathbf{x}}$ is called a spline function, or just a spline, of degree p with knots \mathbf{x} .

Remark 3.3. *By assuming that no knot occurs more than $p + 1$ times, it is possible to prove that $\{B[\mathbf{x}_i]\}_{i=1}^n$ is a basis for $\mathbb{S}_{p,\mathbf{x}}$.*

We can refine a spline curve $f(x) = \sum_{i=1}^n b_i B[\mathbf{x}_i](x)$ by inserting new knots in \mathbf{x} and then computing the coefficients of f in the augmented spline space. An efficient way to perform this process is the *Oslo algorithm* [CLR80].

Lastly, we specify the type of knot vectors we will consider in the next sections, as they allow to define B-spline bases that interpolate the boundaries.

Definition 3.4. A knot vector $\mathbf{x} = [x_1, \dots, x_{n+p+1}]$ is said to be $(p + 1)$ -regular if

1. $n \geq p + 1$,
2. $x_{p+1} < x_{p+2}$ and $x_n < x_{n+1}$,
3. $x_j < x_{j+p+1}$ for $j = 1, \dots, n$,
4. $x_1 = x_{p+1}$ and $x_{n+1} = x_{n+p+1}$.

3.2 Tensor product B-splines

One of the simplest and most straightforward generalization to multiple variables uses tensor products of univariate B-splines.

Definition 3.5 (Bivariate tensor product B-spline). A *bivariate tensor product B-spline* of bi-degree $\mathbf{p} := (p_x, p_y) \in \mathbb{N}^2$ is a separable function $B : \mathbb{R}^2 \rightarrow \mathbb{R}$ defined as

$$B[\mathbf{x}, \mathbf{y}](x, y) := B[\mathbf{x}](x) \cdot B[\mathbf{y}](y), \quad (2)$$

where $\mathbf{x} \in \mathbb{R}^{p_x+2}$ and $\mathbf{y} \in \mathbb{R}^{p_y+2}$ are local knot vectors along x and y .

By assuming that $x_1 < x_{p_x+2}$ and $y_1 < y_{p_y+2}$, it follows that $B[\mathbf{x}, \mathbf{y}]$ is a piecewise polynomial of degree \mathbf{p} .

Definition 3.6 (Bivariate tensor product spline space). A *bivariate tensor product spline space* $\mathbb{S}_{\mathbf{p},[\mathbf{x},\mathbf{y}]}$ is the linear space defined by

$$\mathbb{S}_{\mathbf{p},[\mathbf{x},\mathbf{y}]} := \mathbb{S}_{p_x, \mathbf{x}} \otimes \mathbb{S}_{p_y, \mathbf{y}} = \text{span} \{B[\mathbf{x}_i] \cdot B[\mathbf{y}_j]\}_{i=1, j=1}^{n_1, n_2},$$

where $\mathbf{x} \in \mathbb{R}^{n_x+p_x+2}$ and $\mathbf{y} \in \mathbb{R}^{n_y+p_y+2}$ are global knot vectors. An element $f \in \mathbb{S}_{\mathbf{p},[\mathbf{x},\mathbf{y}]}$ is called a (bivariate) *tensor product spline* function, or just a spline, of bi-degree \mathbf{p} with (global) knot vectors \mathbf{x} and \mathbf{y} .

The tensor product spline representation inherits all the properties (local support, non-negativity, local smoothness) of the univariate case. We refer the reader to [Sch07] for a more exhaustive introduction on B-splines.

3.3 Spline spaces spanned by collections of tensor product B-splines

Traditional B-splines spaces are defined as a tensor product of univariate spline spaces. The advantage of considering a tensor product structure includes the implementation of easy and efficient algorithms for evaluation, simple derivation with respect to any variable and a straightforward generalization of many results of the univariate case. This simple and elegant formulation comes at the cost of a larger amount of data as the size of the problem increases.

Local refinement can be recovered by considering more general collections of tensor product B-splines, which still ensure compatibility with classical tensor-product structures (see Figure 1 for an example of different refinements). The general strategy we will use can be summarized as follows. As a starting point, a coarse tensor product space is considered. Then, a refinement process iterates in a nested sequence of spline spaces, each of which is guaranteed to span the full polynomial space over each element. Examples of spline spaces defined by using this strategy are:

- Hierarchical B-splines [FB88].
- T-splines [SZBN03].
- LR B-splines [DLP13].

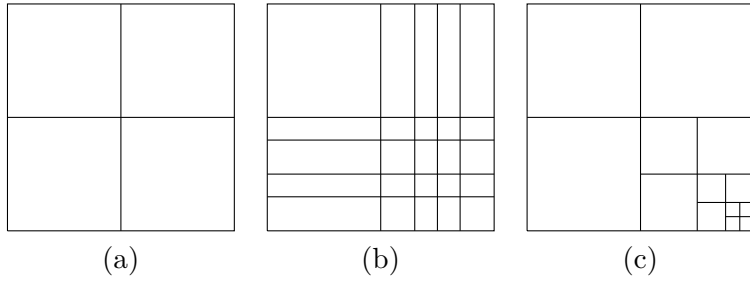


Figure 1: Initial mesh (a), a tensor-product refinement (b) and a truly local refinement in the form of an LR mesh (c).

We will here consider any linearly independent collection of B-splines that can be obtained by means of such a general strategy, with a special attention of LR B-splines. For more details, we refer the reader to [DSB18].

4 A quasi-interpolant spline approach

From the mathematical point of view, every surface can be locally projected onto a plane by using an injective map and, if locally regular, it can be expressed in local coordinates as $(x, y, z(x, y))$. Hence, it is not restrictive to shift the focus to local approximations which will be then glued together, for instance considering a multi-chart decomposition such as [CHCH06].

Quasi-interpolation is a very easy procedure in function approximation theory. The term quasi-interpolation has been interpreted differently according to the context. Cheney [Che95] defines a quasi interpolant as any linear operator L of the form

$$Lf := \sum_{i=1}^{n_x} \sum_{j=1}^{n_y} f(x_i, y_j) g_{i,j}, \quad (3)$$

where $f : \Omega \subset \mathbb{R}^2 \rightarrow \mathbb{R}$ is a function being approximated, $n_x \in \mathbb{N} \cup \{+\infty\} \ni n_y$, (x_i, y_j) are given *nodes* and $g_{i,j} : \Omega \subset \mathbb{R}^2 \rightarrow \mathbb{R}$ are functions at our disposal. Here, we shift focus from a function to a point cloud approximation. The only assumption is that the size of the neighborhood of a point is larger than the sampling density at that point [BTS⁺14].

Definition 4.1. Let $\mathcal{P} \subset \mathbb{R}^3$ be a point cloud and $\mathbf{p} = (p_x, p_y) \in \mathbb{N}^* \times \mathbb{N}^*$ be a bi-degree. Let \mathbf{x} be a $(p_x + 1)$ -regular knot vector with boundary knots $x_{p_x} = a_1$ and $x_{n_x} = b_1$ and let \mathbf{y} be a $(p_y + 1)$ -regular knot vector with boundary knots $y_{p_y} = a_2$ and $x_{n_y} = b_2$. The

Weighted Quasi Interpolant Spline Approximation of bi-degree \mathbf{p} to the point cloud \mathcal{P} over the knot vectors \mathbf{x} and \mathbf{y} is defined by

$$f_w(x, y) := \sum_{i=1}^{n_x} \sum_{j=1}^{n_y} \hat{z}_w(x_i^*, y_j^*) \cdot B[\mathbf{x}_i, \mathbf{y}_j](x, y), \quad (4)$$

where $x_i^* := (x_i + \dots + x_{i+p_x})/p_x$ and $y_j^* := (y_j + \dots + y_{j+p_y})/p_y$ are the *knot averages* and the expression

$$\hat{z}_w(u, v) := \frac{\sum_{(x,y,z) \in \mathcal{P}} z \cdot w(x, y, u, v)}{\sum_{(x,y,z) \in \mathcal{P}} w(x, y, u, v)}$$

is the *control points estimator* of weight function $w : \mathbb{R}^2 \times \mathbb{R}^2 \rightarrow [0, 1]$.

The function w defines a *window* around each point and is sometimes called a *Parzen window*. An example is the weight function

$$w(x, y, u, v) := \begin{cases} 1/k, & \text{if } (x, y) \in N_k(u, v) \\ 0, & \text{otherwise} \end{cases},$$

where $k \in \mathbb{N}^*$ and $N_k(u, v)$ denotes the neighborhood of (u, v) defined by the k closest points of the point cloud. In this case, \hat{z}_w defines the k -nearest neighbor estimator (see Figure 4). Commonly the function w depends on the distance $\|(x, y) - (u, v)\|_2$, for examples:

$$w(x, y, u, v) = \mathbb{1}_{\|(x-u, y-v)\|_2 \leq r} \quad (\text{Characteristic}) \quad (5a)$$

$$w(x, y, u, v) = e^{-\|(x-u, y-v)\|_2/2\sigma^2} \quad (\text{Gaussian}) \quad (5b)$$

$$w(x, y, u, v) = e^{-\|(x-u, y-v)\|_2/\sqrt{2}\sigma} \quad (\text{Exponential}) \quad (5c)$$

Notice that w depends on the knot averages, and can thus be adapted to local information (e.g. variable level and/or nature of noise).

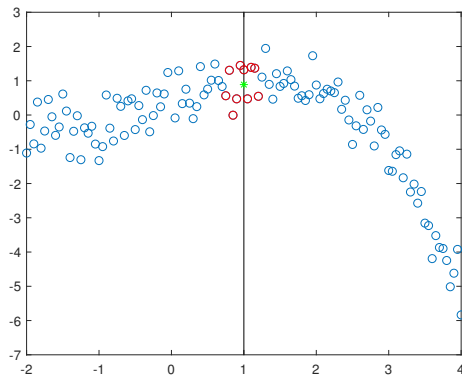


Figure 2: Given a 2D point cloud (in blue) and the axis $x = 1$, we use the 10-nearest neighbors (in red) to compute an estimation (in green).

4.1 Properties

The weighted quasi interpolant spline approximation is a very simple and robust procedure to obtain a spline approximation of point clouds. As in the original method for function approximations, it preserves interesting properties under mild assumptions. For examples, if the points have all positive heights, then the spline approximation will also be positive. We now list some relevant theoretical results.

Local representation

Let $x \in [x_\mu, x_{\mu+1})$ for some μ in the range $p_x + 1 \leq \mu \leq n_x$ and $y \in [y_\nu, y_{\nu+1})$ for some ν in the range $p_y + 1 \leq \nu \leq n_y$. By using the property of local support for B-splines (see Figure 3 for an example), Equation 4 can be reduced to

$$f_w(x, y) := \sum_{i=\mu-p_x}^{\mu} \sum_{j=\nu-p_y}^{\nu} \hat{z}_w(x_i^*, y_j^*) \cdot B[\mathbf{x}_i, \mathbf{y}_j](x, y). \quad (6)$$

Thus, the approximation on $[x_\mu, x_{\mu+1}) \times [y_\nu, y_{\nu+1})$ only depends on $(p_x + 1)(p_y + 1)$ coefficients, which are computed by using the (sub-) point cloud:

$$\mathcal{P}_{\mu, \nu} := \bigcup_{\substack{i=\mu-p_x, \dots, \mu \\ j=\nu-p_y, \dots, \nu}} \left\{ \text{supp} \left(w(\cdot, \cdot, x_i^*, y_j^*) \right) \right\} \cap \mathcal{P}.$$

Notice that the set of points which are effectively used to compute the approximation, i.e.

$$\mathcal{P}^* := \bigcup_{\substack{\mu=p_x+1, \dots, n_x \\ \nu=p_y+1, \dots, n_y}} \mathcal{P}_{\mu, \nu}$$

may be a proper subset of \mathcal{P} .

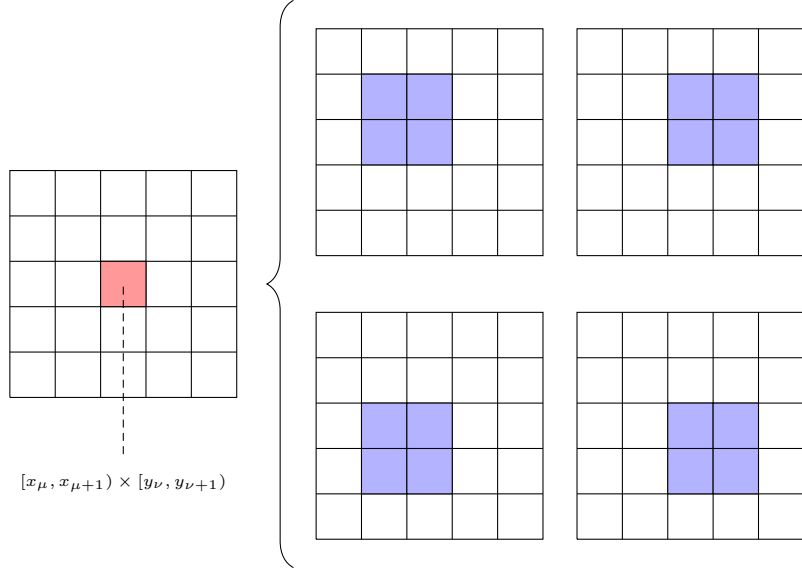


Figure 3: Local support of a B-spline. Given a tensor product mesh for the spline space of bi-degree $(1, 1)$, there are exactly four B-splines (in light-blue) containing a chosen element (in light-red) inside their support.

Global and local bounds

- *Global bounds.* Let $\mathcal{P} \subset \mathbb{R}^3$ be a point cloud and $z_{\min}, z_{\max} \in \mathbb{R}$ that satisfy

$$z_{\min} \leq z \leq z_{\max}, \quad \text{for all } (x, y, z) \in \mathcal{P}.$$

Then the weighted quasi interpolant spline approximation to \mathcal{P} from some spline space $\mathbb{S}_{p, [\mathbf{x}, \mathbf{y}]}$ and some weight function w has the same (global) bounds

$$z_{\min} \leq f_w(x, y) \leq z_{\max}, \quad \text{for all } (x, y) \in \mathbb{R}^2. \quad (7)$$

- *Local bounds.* Let $x \in [x_\mu, x_{\mu+1})$ for some μ in the range $p_x + 1 \leq \mu \leq n_x$ and $y \in [y_\nu, y_{\nu+1})$ for some ν in the range $p_y + 1 \leq \nu \leq n_y$. The global bounds of Equation 7 can be refined, by using the local representation of Equation 6, to

$$\min_{\substack{i=\mu-p_x, \dots, \mu \\ j=\nu-p_y, \dots, \nu}} \hat{z}_w(x_i^*, y_j^*) \leq f_w(x, y) \leq \max_{\substack{i=\mu-p_x, \dots, \mu \\ j=\nu-p_y, \dots, \nu}} \hat{z}_w(x_i^*, y_j^*). \quad (8)$$

We can simplify these bounds to

$$\min \left\{ z \text{ s.t. } (x, y, z) \in \mathcal{P}_{\mu, \nu} \right\} \leq f_w(x) \leq \max \left\{ z \text{ s.t. } (x, y, z) \in \mathcal{P}_{\mu, \nu} \right\}.$$

by using the following geometric argument:

- Since \hat{z}_w is defined by a convex combination, each point $(x_i^*, y_j^*, z_w(x_i^*, y_j^*))$ belongs to the convex hull generated by \mathcal{P} .
- As observed in the previous section, the point cloud that defines f_w over $[x_\mu, x_{\mu+1}) \times [y_\nu, y_{\nu+1})$ is $\mathcal{P}_{\mu, \nu} \subseteq \mathcal{P}^* \subseteq \mathcal{P}$, and therefore $(x_i^*, y_j^*, z_w(x_i^*, y_j^*))$ belongs to the convex hull generated by $\mathcal{P}_{\mu, \nu}$ for any $i = \mu - p_x, \dots, \mu$ and $j = \nu - p_y, \dots, \nu$.

Special configurations

If $x_{i+1} = \dots = x_{i+p_x} < x_{i+p_x+1}$ and $y_{j+1} = \dots = y_{j+p_y} < y_{j+p_y+1}$ then

$$f_w(x_i^*, y_j^*) = \hat{z}(x_i^*, y_j^*).$$

Thus, by using knots of maximum multiplicity, our approximation interpolates the control net $\{\hat{z}(x_i^*, y_j^*)\}_{i,j}$. Notice moreover that, by assuming w to be a 1-NN weight function:

- if the point cloud consists of measurements at the knot averages, then f_w provides its interpolation.
- if the point cloud consists of samplings of a continuous function $f : [a_1, b_1] \times [a_2, b_2] \rightarrow \mathbb{R}$ at the knot averages, then f_w is known as *Variation Diminishing Spline Approximation* (see [LM11] for more details).

Shape preservation

As pointed out by Goodman [Goo89], certain shape preserving properties of a tensor product spline representation follow easily from the corresponding properties of the respective univariate spline spaces. In our case:

- *Preservation of monotonicity.* If $\hat{z}_w(x_i^*, y_j^*)$ is an increasing sequence for each j , then it follows that f_w is an increasing function of x for each y . Similarly, by assuming that $\hat{z}_w(x_i^*, y_j^*)$ is an increasing sequence for each i , it follows that f_w is an increasing function of y for each x . If both these hold then $f_w(x_1, y_1) \leq f_w(x_2, y_2)$ for all $(x_1, y_1), (x_2, y_2)$ such that $x_1 \leq x_2$ and $y_1 \leq y_2$.
- *Preservation of convexity.* Suppose that

$$\Delta_x \hat{z}_w(x_i^*, y_j^*) := p_x \frac{\hat{z}_w(x_i^*, y_j^*) - \hat{z}_w(x_{i-1}^*, y_j^*)}{x_{i+p_x} - x_i}$$

is an increasing sequence for each j , then it follows that f_w is a convex function of x for each y . A similar argument can be applied to show the preservation of convexity of y for each x .

For more details we refer again the reader to [LM11].

4.2 A learning approach to refinement

The purpose of a refinement approach is to enrich the function space until the desired approximation accuracy is reached. The use of a hierarchy of lattices, although theoretically simple, turns out to be computationally inefficient as the data size increases [LWS97].

The local quality of an approximation can be used to refine only those regions where an higher precision is needed. Once a first approximation on an initial tensor product mesh has been computed, a local refinement can be performed where the approximation is not accurate enough. As stated in [RBD⁺17], this allows to

- *Keep the degree low.* A low degree is useful both from a computational (numerical stability, computational complexity,...) and from a geometric viewpoint (problem of extra branches when the degree is "high").
- *Add degrees of freedom where they are needed.* The ability to refine locally ensures that the degrees of freedom are present in the area of interest (again: numerical stability, computational complexity,...).
- *Guarantee watertight models.* Three-dimensional models may be affected by small gaps. In applications such as CAD and 3D printing, a better model is required.

The quality of a surface approximation relies on its prediction capability on independent points. In a data-rich situation, we can partition the point set into three parts:

- *Training point cloud.* Used to compute the coefficients for the quasi-interpolant.
- *Validation point cloud.* Used to estimate some prediction error for model selection (e.g. to choose a k in a k -NN estimation of the control net or to quantify the accuracy of the approximation on different meshes).
- *Test point cloud.* Used to assess the generalization performances on an independent set.

Note that the three point sets must be, whether used, representative of the original shape [HTF09]. An example is shown in Figure 4.

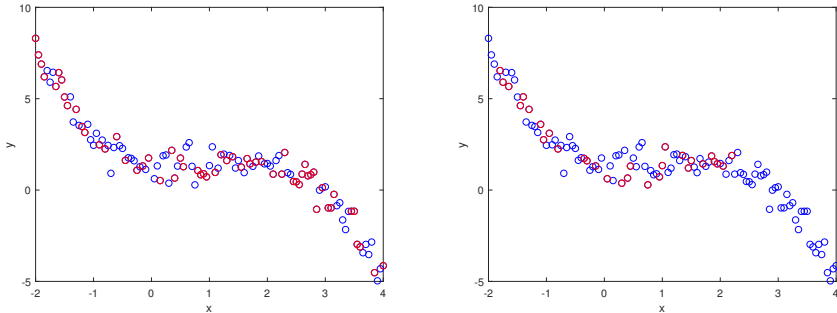


Figure 4: Sampling representativeness. Left, a given point cloud (in blue) and a representative downsampling (in red). Right, the same point cloud (in blue) and a non representative downsampling (in red)

Efficient examples of sample re-use, suitable to get results independently on the chosen partition, are cross-validation and the bootstraps methods. A simplified scheme of the refinement process is depicted in Figure 5. A sketch of the algorithm is provided in Algorithm 1.

Algorithm 1 Iterative w-QISA

Input: A point cloud \mathcal{P} .
A weight function $w : \mathbb{R}^2 \times \mathbb{R}^2 \rightarrow [0, 1]$.
An initial tensor mesh \mathcal{M}_0 .

Output: A piecewise polynomial approximation.

/*(Optional) point cloud partitioning*/

- 1: Partition \mathcal{P} in the three sub-point clouds $\mathcal{P}_{\text{training}}$, $\mathcal{P}_{\text{validation}}$, $\mathcal{P}_{\text{test}}$.
- /*Iteration 0 (tensor mesh)*/
- 2: Let \mathcal{V}_0 denote the collection of tensor product B-splines on \mathcal{M}_0 .
- 3: Let \mathcal{E}_0 denote the collection of (minimal) elements on \mathcal{M}_0 .
- 4: Compute $f_w^{(0)} \in \text{span}(\mathcal{V}_0)$ from $\mathcal{P}_{\text{training}}$ by Equation 4.
- 5: Compute a local error $E_0 : \mathcal{E}_0 \rightarrow [0, +\infty)$ on $\mathcal{P}_{\text{validation}}$.
- /*Iteration $n \in \mathbb{N}^*$ (local refinement)*/
- 6: **while** $f_w^{(n)}$ does not satisfy the accuracy test **do**
- 7: Set $n=n+1$.
- 8: (Locally) refine \mathcal{M}_{n-1} into \mathcal{M}_n .
- 9: Let \mathcal{V}_n be the collection of tensor product B-splines on \mathcal{M}_n .
- 10: Let \mathcal{E}_n denote the collection of (minimal) elements on \mathcal{M}_n .
- 11: Compute $f_w^{(n)} \in \text{span}(\mathcal{V}_n)$ from $\mathcal{P}_{\text{training}}$ by Equation 4.
- 12: Compute a local error $E_n : \mathcal{E}_n \rightarrow [0, +\infty)$ on $\mathcal{P}_{\text{validation}}$.
- 13: Compute a global error on $\mathcal{P}_{\text{test}}$.
- 14: **Return** $f_w = f_w^{(n)}$.

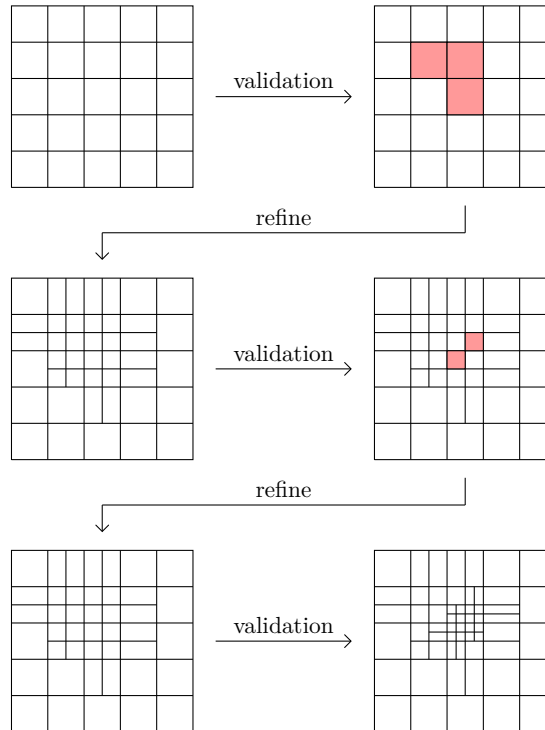


Figure 5: Iterative local refinement. An initial tensor product mesh (top-left) is considered to approximate a given 3D (training) point cloud. At each iteration, a validation of the approximation determines which elements, represented in light-red (if any), need to be (locally) refined.

The computational complexity of our approach mainly depends on the chosen control net estimators. In case of a k -NN weight, the time needed to compute a single coefficient is proportional to $O(k \log(N))$, where N is the number of points. To further reduce the computational complexity of the k -NN search, it is possible to follow the k-d trees approach proposed in [GCSA13].

5 Numerical simulation

The weighted quasi-interpolant spline approximation represents a valid technique for surface fitting problems. The key idea is the definition of a quasi-interpolant such that the computation of the control net has a reduced computational complexity when compared to the traditional methods. In this section, we test our method both to synthetic and real data. We use the implementation of LR B-splines proposed in [SD19].

5.1 Preliminary tests on simulated data

We present two examples of simulated data, with the purpose of emphasizing the strengths and the limits of our method. First, we start from a low-noise point cloud, which allows us to show that the shape preservation conditions of Section 4.1 are not so restrictive when the data are not extremely perturbed. Then, we increasingly perturb a simpler shape by noise and outliers in order to numerically test stability and robustness.

Approximation of a low-noise complex shape

As a sanity check we apply our technique on a low Gaussian-noise point set. The data are generated by sampling the function $g_1 : [-3, 3] \times [-3, 3] \rightarrow \mathbb{R}$ defined by

$$g_1(x, y) := \frac{\sin(2x^2 + y^2 + e)}{2x^2 + y^2 + e} + \frac{\sin(x^2 + 2y^2 + e)}{x^2 + 2y^2 + e}.$$

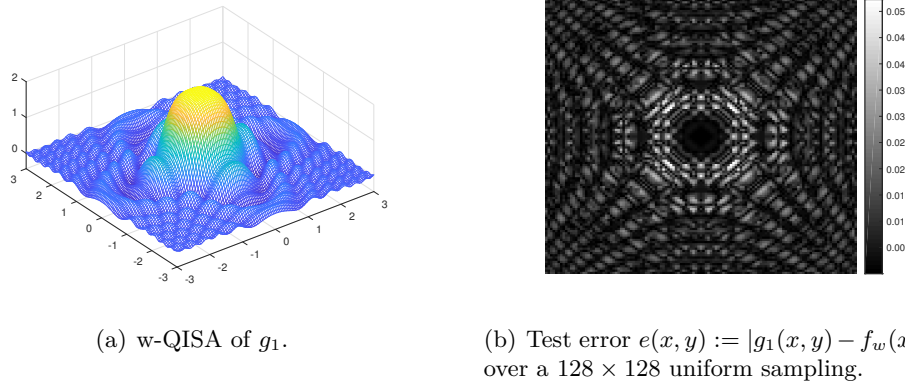


Figure 6: Approximation of a noisy point cloud sampled from the analytic function g_1 .

The chosen function is analytic, hence smooth. The quick change of monotonicity and convexity, together with its positivity, make g_1 an interesting candidate to show how a good approximation can be computed without giving up too much geometric information. We choose to combine a Gaussian weight function (see Equation 5b) with a k -NN weight function:

$$w(x, y, u, v) := \begin{cases} e^{-\|(x-u, y-v)\|_2}, & \text{if } (x, y) \in N_k(u, v) \\ 0, & \text{otherwise} \end{cases},$$

as this allows to define a smoother for Gaussian noise which has also local support. A C^1 biquadratic approximation is computed from an initial regular tensor mesh. Figure 6 illustrates the final approximation and the test error in the form of a bidimensional image. Our simulation shows that, for the chosen weight function, continuity and convexity of the initial function are preserved. The positivity of the input point set is translated into the positivity of the final approximation. The local shape control ensures an increased precision in proximity of the boundary of the domain, where fluctuations are more frequent. Lastly, the use of knot ends having maximum multiplicity guarantees interpolation of the estimated control net at the boundaries.

Approximation of an increasingly perturbed simple shape

Compared to traditional MBA approximations, our approach is strongly resistant to both noise and outliers. Let $g_2 : [0, 3] \times [0, 3] \rightarrow \mathbb{R}$ be the sum of Gaussians defined by

$$g_2(x, y) := \sum_{k=0}^2 \exp \left(- \left(\frac{(x - x_k)^2}{2\sigma_x^2} + \frac{(y - y_k)^2}{2\sigma_y^2} \right) \right),$$

where $(x_k, y_k) := (1 + 0.5 \cdot k, 1 + 0.5 \cdot k)$ for any $k = 0, 1, 2$, $\sigma_x := 0.8 =: \sigma_y$. Figure 7 presents the approximation of a point cloud, initially sampled from the surface and then perturbed by uniform noise and outliers, by a C^1 biquadratic spline. Notice the

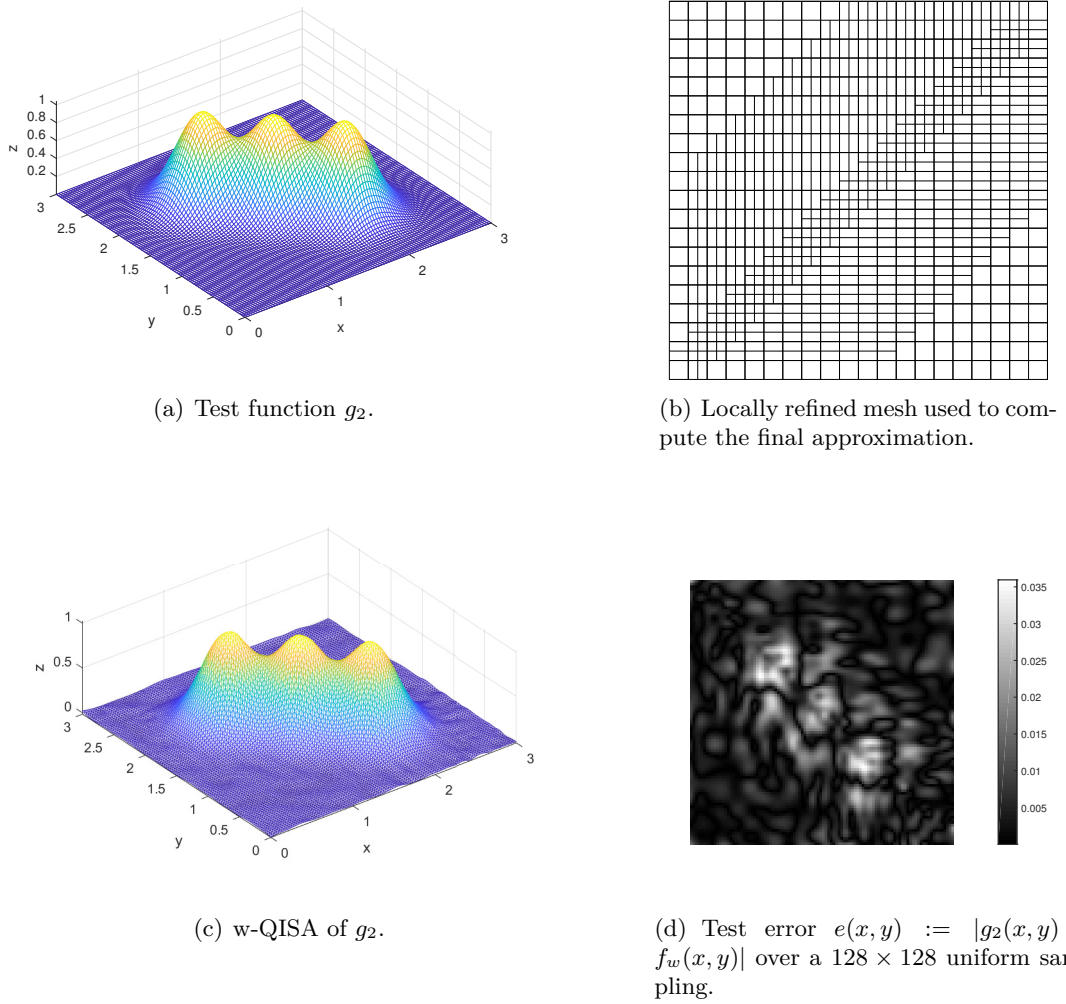


Figure 7: Approximation of a noisy point cloud sampled from the analytic function g_2 .

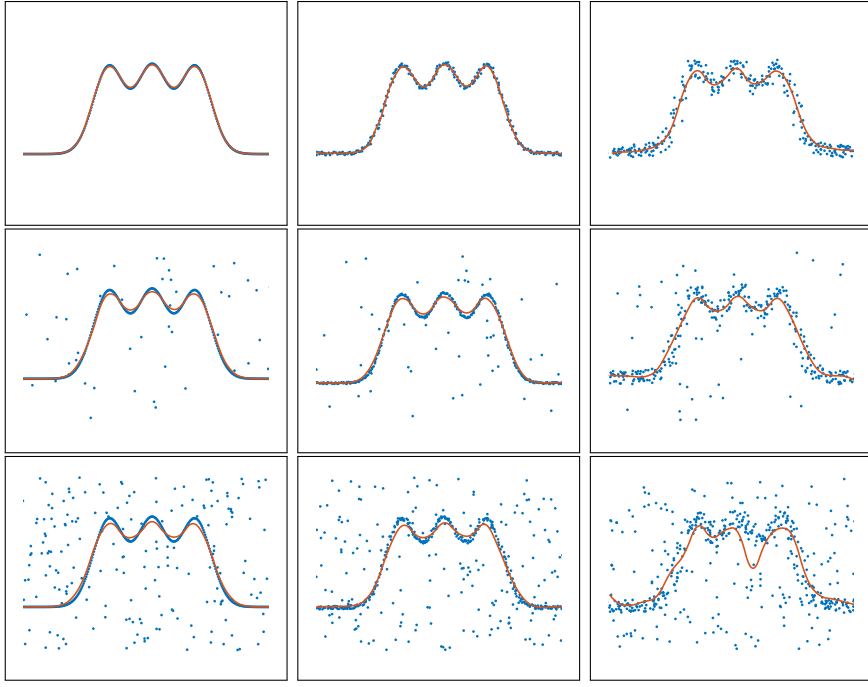


Figure 8: Noise and outliers robustness. The noise increases from the left to the right. The outliers increase from top to bottom.

use of a local refinement, which allows to reduce the chosen validation error below a given threshold without adding unnecessary degrees of freedom. Figure 8 illustrates the stability of our method (until failure) against increasing amount of noise and outliers. In both simulations, a k -NN weight is filtered from outliers by using quartiles.

5.2 Simulation on real data

We now consider several real data as representatives of both different data collections and application domains.

An artifact from the STARC repository

A first model comes from the Science and Technology in Archaeology Research Center (STARC, [STA]) of The Cyprus Institute. Figure 9 graphically compares the original point cloud, in particular a user-selected region (in green) and the final approximation. Given the unknown nature of the noise, a pure k -NN weight function is here tested.



Figure 9: Original model (from STARC repository [STA]) (left) and local reconstruction (right).

The approximation shows a correct recovery of the main details of the artefact, with an accurate shape preservation. Nevertheless, the feeble details are lost, sign that this weight function has a smoothing effect. Lastly, the symmetry of the bulge at the center of the spiral is maintained.

A bust of Queen Nefertiti

We then test a more complex shape. We consider “The Other Nefertiti”, an artistic intervention by the two German artists Nora Al-Badri and Jan Nikolai Nelles. The 3D triangulated mesh represents the bust of Queen Nefertiti (Nofretete), one of the top attractions of the Egyptian Collection in the neues Museum on Berlin’s Museum Island. Local approximations of the face and of a detail of the hat are provided in Figure 10. As for the previous example, we choose to compute a C^1 biquadratic spline approximation, with control net estimated through a k -NN weight function.

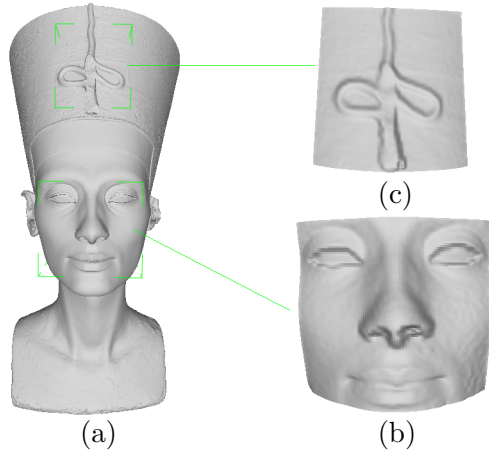


Figure 10: (a) A 3D model and (b,c) two details on the local approximation.

A fringe decoration

The method provides a faithful reconstruction even in presence of small geometric variations, such as chiselings or local reliefs. Figure 11 illustrates a local reconstruction of a fragment of a votive statuette from the STARC repository. We graphically compare how a local detail is approximated by a w -QISA, with k -NN weight function, and a Poisson reconstruction. As shown in the picture, the visual impression is comparable.

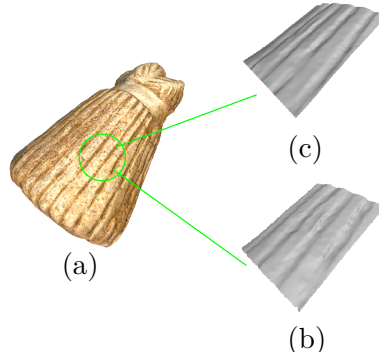


Figure 11: (a) A 3D model, together with a local comparison between (b) a Poisson reconstruction and (c) a w -quasi interpolant spline approximation.

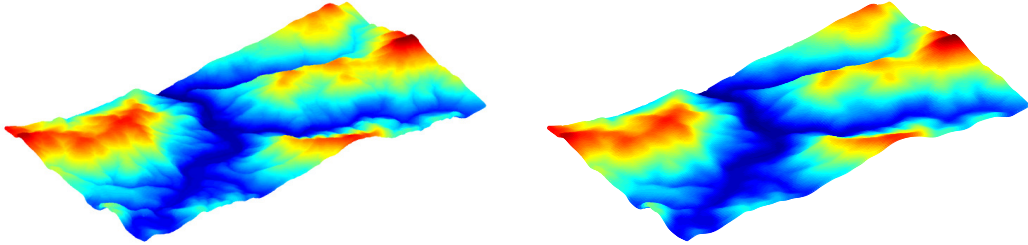


Figure 12: Santo Stefano d’Aveto, Liguria, Italy. Left: data point cloud from the given region of interest. Right: 5-NN quasi-interpolant spline approximation. The colors represent the elevation and vary from blue (low elevation) to red (high elevation).

Terrain data

A simulation on scattered terrain data is shown in Figure 12. The data are part of the Liguria-LAS dataset adopted as testbed in the iQmulus project [EC 16], and come from a LIDAR dataset with spatial resolution of one meter. The area here selected contains 468120 points. It is located in the Liguria region, in the north-west of Italy. Liguria corresponds to a long and narrow strip of land, squeezed between the sea, the Alps and the Apennines mountains. Its morphology, with several small catchments and even small rivers, is very challenging for the approximation methods to capture and preserve the most important and potentially critical characteristics. The data are not post-processed, thus they contain noise and outliers. We choose a C^1 biquadratic surface as they are smooth enough to represent smooth terrains in a good way.

6 Conclusion and future work

We presented a novel quasi-interpolant reconstruction technique, specifically designed to handle large and noisy point sets, even when equipped of outliers. The robustness and the versatility of the method are theoretically proved in Section 4 and tested over point clouds from different origins in Section 5. The definition of the control point estimators combines the computational efficiency with the possibility to work with different families of noise, as well as a reduced sensitivity to outliers. The computational complexity is, in fact, comparable to that of the control net estimation. Tensor product approximations preserve shape information such as monotonicity and convexity. Compared to other approaches, such as tensor product approximations, the number of degrees of freedom is here reduced via the local refinement: a general quantification of this reduction is however impossible, as the number of degrees of freedom depends more on the characteristic of the data than on the number of points of the dataset.

To the best of our knowledge, this work presents the first quasi-interpolant scheme that applies a local refinement robust to noise and outliers to point clouds, in particular adopting the LR B-spline scheme. This is particularly relevant because LR B-splines naturally deal with isogeometric computations and simulation and offers the valuable perspective to practically adopt this work for Computer Aided Design and Manufacturing (CAD/CAM), Finite Element Analysis and IsoGeometric Analysis [JKD14, OEBM19].

As future perspectives, we plan to extend this model to hypersurfaces of \mathbb{R}^d , with the purpose of introducing a more general approach that can be seen as a regression method of statistical learning. Moreover, having a local support, our method looks easily parallelizable, for instance adopting a zonal grid embedding, thus paving the way to realistic engineering simulations.

Acknowledgments

This project has received funding from the European Union’s Horizon 2020 research and innovation programme under the Marie Skłodowska-Curie grant agreement No 675789. Dott. S. Biasotti work has been partially supported by the EU ERC Advanced Grant CHANGE, grant agreement No. 694515 and the CNR-IMATI project DIT.AD021.080.001. The authors also thanks: Dr. Bianca Falcidieno and Dr. Michela Spagnuolo for the fruitful discussions; Dr. Oliver J. D. Barrowclough, Dr. Tor Dokken and Dr. Georg Muntingh for their concern as supervisors; Eng. Simone Cammarasana for his help in the figures generation.

References

- [ABCO⁺01] M. Alexa, J. Behr, D. Cohen-Or, S. Fleishman, D. Levin, and C.T. Silva. Point set surfaces. In *Proceedings of the conference on visualization 01, VIS 01, IEEE Computer Society*, pages 21–28, 2001.
- [AG15] J. Ackermann and M. Goesele. A survey of photometric stereo techniques. *Foundations and Trends in Computer Graphics and Vision*, 9(3–4):149–254, 2015.
- [AK04] N. Amenta and Y.J. Kil. Defining point-set surfaces. In *ACM SIGGRAPH 2004 papers, ACM*, pages 264–270, 2004.
- [BBCS99] F. Bernardini, C. L. Bajaj, J. Chen, and D. Schikore. Automatic reconstruction of 3D CAD models from digital scans. *International Journal of Computational Geometry & Applications*, 9(4):327–369, 1999.
- [BBX95] C. L. Bajaj, F. Bernardini, and G. Xu. Automatic reconstruction of surfaces and scalar fields from 3D scans. In *Proceedings of ACM SIGGRAPH 95*, pages 109–118, 1995.
- [BD12] O. J. D. Barrowclough and T. Dokken. Approximate implicitization using linear algebra. *Journal of Applied Mathematics*, 2012.
- [Bli82] J. F. Blinn. A generalization of algebraic surface drawing. In *ACM Transactions on Graphics 1, 3*, pages 235–256, 1982.
- [BTS⁺14] M. Berger, A. Tagliasacchi, L. Seversky, P. Alliez, J. Levine, A. Sharf, and C. Silva. State of the Art in Surface Reconstruction from Point Clouds. In *Eurographics STAR (Proc. of EG’14)*, 2014.
- [CBC⁺01] J. C. Carr, R. K. Beatson, J. B. Cherrie, T. J. Mitchell, W. R. Fright, B. C. McCallum, and T. R. Evans. Reconstruction and representation of 3D objects with radial basis functions. In *n Proceedings of ACM SIGGRAPH 2001*, pages 67–76, 2001.
- [CHCH06] N. A. Carr, J. Hoberock, K. Crane, and J. C. Hart. *Rectangular Multi-chart Geometry Images*, pages 181–190. Eurographics Association, 2006.
- [Che95] E. W. Cheney. *Approximation Theory, Wavelets and Applications*, volume 454, chapter Quasi-interpolation, pages 37–45. Springer. NATO Science Series (Series C: Mathematical and Physical Sciences), 1995.
- [CL96] B. Curless and M. Levoy. A volumetric method for building complex models from range images. In *Proceedings of ACM SIGGRAPH 1996*, pages 303–312, 1996.

[CLR80] E. Cohen, T. Lyche, and R. R. Riesenfeld. Discrete b-splines and subdivision techniques in computer-aided design and computer graphics. *Computer Graphics & Image Processing*, 14(2):87–111, 1980.

[DLP13] T. Dokken, T. Lyche, and K. F. Pettersen. Polynomial splines over locally refined box-partitions. *Computer Aided Geometric Design*, 30(3):331–356, 2013.

[Dok96] T. Dokken. *Aspects of Intersection Algorithms and Approximation*. PhD thesis, University of Oslo, 1996.

[DSB18] T. Dokken, V. Skytt, and O. Barrowclough. Trivariate spline representations for computer aided design and additive manufacturing. *Computer & Mathematics with Applications*, 2018.

[DST01] H. Q. Dinh, G. Slabaugh, and G. Turk. Reconstructing surfaces using anisotropic basis functions. In *International Conference on Computer Vision (ICCV) 2001*, pages 606–613, 2001.

[EC 16] EC IST. FP7 Integrating Project: IQmulus. <http://www.iqmulus.eu/>, 2012–2016. contract number.

[FB88] D. R. Forsey and R. H. Bartels. Hierarchical b-spline refinement. *ACM SIGGRAPH Computer Graphics*, pages 205–212, 1988.

[FC11] G. Taubin F. Calakli. Ssd: Smooth signed distance surface reconstruction. *Computer Graphics Forum*, 2011.

[FCOS05] S. Fleishman, D. Cohen-Or, and C.T. Silva. Robust moving least-squares fitting with sharp features. In *ACM SIGGRAPH 2005 papers*, ACM, pages 544–552, 2005.

[FYD14] W. Feng, Z. Yang, and J. Deng. Moving multiple curves/surfaces approximation of mixed point clouds. *Commun Math Stat*, 2(1):107–124, 2014.

[GCSA13] Simon Giraudot, David Cohen-Steiner, and Pierre Alliez. Noise-adaptive shape reconstruction from raw point sets. *Proceedings of the Eleventh Eurographics/ACMSIGGRAPH Symposium on Geometry Processing*, pages 229–238, 2013.

[Geo17] A. Georgopoulos. *Heritage and Archaeology in the DigitalAge*. Springer, 2017.

[Goo89] T. N. T. Goodman. Shape preserving representations. *Mathematical Methods in Computer Aided Geometric Design*, pages 333–351, 1989.

[HDD⁺92] H. Hoppe, T. DeRose, T. Duchamp, J. McDonald, and W. Stuetzle. Surface reconstruction from unorganized points. In *Proceedings of the 19th annual conference on computer graphics and interactive techniques*, ACM, pages 71–78, 1992.

[HTF09] T. Hastie, R. Tibshirani, and J. Friedman. *The Elements of Statistical Learning*. Springer, second edition, 2009.

[JF02] B. Jüttler and A. Felis. Least-squares fitting of algebraic spline surfaces. *Adv. Comput. Math.*, 17(1-2):135–152, 2002.

[JKD14] K. A. Johannessen, T. Kvamsdal, and T. Dokken. Isogeometric analysis using lr b-splines. *Computer Methods in Applied Mechanics and Engineering*, 2014.

[KBH06] M. Kazhdan, M. Bolitho, and H. Hoppe. Poisson surface reconstruction. In *Proceedings of the fourth eurographics symposium on geometry processing, Eurographics Association*, pages 61–70, 2006.

[KH13] M. Kazhdan and H. Hoppe. Screened poisson surface reconstruction. In *ACM Transactions on Graphics*, 2013.

[KHS03] K. Kojekine, I. Hagiwara, and V. Savchenko. Software tools using CSRBFs for processing scattered data. *Computers & Graphics*, 23(2), April 2003.

[LA13] F. Lafarge and P. Alliez. Surface reconstruction through point set structuring. *Computer Graphics Forum (Proc. of Eurographics)*, 2013.

[Lev03] D. Levin. *Geometric modeling for scientific visualization*, chapter Mesh-independent surface interpolation, pages 37–49. Springer-Verlag, 2003.

[LM11] T. Lyche and K. Mørken. *Spline Methods Draft*, chapter Tensor Product Spline Surfaces, pages 149–166. Centre of Mathematics for Applications, University of Oslo, April 2011.

[LTGS95] C. Lim, G. M. Turkiyyah, M. A. Ganter, and D. W. Storti. Implicit reconstruction of solids from cloud point sets. In ACM Press, editor, *Proceedings of the third ACM symposium on Solid Modeling and Applications*, pages 393–402, 1995.

[LWS97] S. Lee, G. Wolberg, and S. Y. Shin. Scattered data interpolation with multilevel b-splines. *IEEE Transactions on Visualization and Computer Graphics*, 3(3):228–244, 1997.

[MGDCS10] P. Mullen, F. D. Goes, M. Desbrun, and D. Cohen-Steiner. Signed the unsigned: robust surface reconstruction from raw pointsets. In *Symp. on Geometry Processing*, pages 1733–1741, 2010.

[Mur91] S. Muraki. Volumetric shape description of range data using blobby model. In *Proceedings of the 18th annual conference on computer graphics and interactive techniques, ACM*, pages 227–235, 1991.

[MYR⁺01] B. S. Morse, T. S. Yoo, P. Rheingans, D. T. Chen, and K. R. Subramanian. Interpolating implicit surfaces from scattered surface data using compactly supported radial basis functions. In *Shape Modeling International 2001*, pages 89–98, 2001.

[NOS09] Y. Nagai, Y. Ohtake, and H. Suzuki. Smoothing of partition of unity implicit surfaces for noise robust surface reconstruction. *Computer Graphics Forum*, 28:1339–1348, 2009.

[OBA⁺03] Y. Ohtake, A. Belyaev, M. Alexa, G. Turk, and H.-P. Seidel. Multi-level partition of unity implicits. In *ACM SIGGRAPH 2003 papers, ACM*, pages 463–470, 2003.

[OBS05] Y. Ohtake, A. G. Belyaev, and H. P. Seidel. 3D scattered data interpolation and approximation with multilevel compactly supported RBFs. *Graphical Models*, 67(3):150–165, 2005.

[OEBM19] M. Occelli, T. Elguedj, S. Bouabdallah, and L. Morançay. LR B-Splines implementation in the Altair RadiossTM solver for explicit dynamics Iso-Geometric Analysis. *Advances in Engineering Software*, 3 2019.

[PASS95] A. Pasko, V. Adzhiev, A. Sourin, and V. Savchenko. Function representation in geometric modelling: concepts, implementation and applications. *The Visual Computer*, 11(8):429–446, 1995.

[PCS⁺17] G. Patané, A. Cerri, V. Skytt, S. Pittaluga, S. Biasotti, D. Sobrero, T. Dokken, and M. Spagnuolo. Comparing methods for the approximation of rainfall fields in environmental applications. *ISPR Journal of Photogrammetry and Remote Sensing*, 127:57–72, 2017.

[Pra87] V. Pratt. Direct least-squares fitting of algebraic surfaces. In *ACM SIGGRAPH Comput Graph*, volume 21, pages 145–152, 1987.

[PVFA10] A. Pasko, T. Vilbrandt, O. Fryazinov, and V. Adzhiev. Procedural Function-based Spatial Microstructures. In *2010 Shape Modeling International Conference*, 2010.

[RBD⁺17] A. Raffo, O. J. D. Barrowclough, H. E. I. Dahl, T. Dokken, M. S. Floater, and G. Muntingh. Locally refined approximate implicitisation for design and manufacturing. *Poster presented at the ARCADES Doctoral School I: Foundations of CAD, Oslo*, 2017.

[RBM18] A. Raffo, O. J. D. Barrowclough, and G. Muntingh. Reverse engineering of CAD models via clustering and approximate implicitization, 2018.

[RS11] M. Rouhani and A. D. Sappa. Implicit B-spline fitting using the 3L algorithm. In *18th IEEE international conference on image processing, ICIP, IEEE*, pages 893–896, 2011.

[RSB15] M. Rouhani, A.D. Sappa, and E. Boyer. Implicit B-spline surface reconstruction. In *IEEE Trans Image Process*, volume 24, pages 22–32, 2015.

[SBD15] V. Skytt, O. Barrowclough, and T. Dokken. Locally refined spline surfaces for representation of terrain data. *Computer & Graphics*, 49:58–68, 2015.

[Sch07] L. L. Schumaker. *Spline Functions: Basic Theory*. Cambridge University Press, 2007.

[SD19] I. Stangeby and T. Dokken. Properties of Spline Spaces Over Structured Hierarchical Box Partitions, 2019.

[Sed85] T. W. Sederberg. Piecewise algebraic surface patches. *Computer Aided Geometric Design*, 2(1-3):53–59, 1985.

[SOS04] C. Shen, J.F. O'Brien, and J.R. Shewchuk. Interpolating and approximating implicit surfaces from polygon soup. In *ACM SIGGRAPH 2004 papers, ACM*, pages 896–904, 2004.

[SPOK95] V. V. Savchenko, A. A. Pasko, O. G. Okunev, and T. L. Kunii. Function representation of solids reconstructed from scattered surface points and contours. In *Computer Graphics Forum*, volume 14, pages 181–188, 1995.

[STA] STARC repository. <http://public.cyi.ac.cy/starcRepo/>.

[STW⁺06] M. F. Shalaby, J. B. Thomassen, E. M. Wurm, T. Dokken, and B. Jüttler. *Algebraic Geometry and Geometric Modeling*, chapter Piecewise approximate implicitization: experiments using industrial data, pages 37–51. Springer Berlin Heidelberg, 2006.

[SZBN03] T. W. Sederberg, J. Zheng, A. Bakenov, and A. Nasri. T-splines and t-nurccs. *ACM Transactions on Graphics*, 22(3):477–484, 2003.

[Tau91] R. Taubin. Estimation of planar curves, surfaces and nonplanar space curves defined by implicit equations with applications to edge and range image segmentation, 1991.

[TO02] G. Turk and J. O’Brien. Modelling with implicit surfaces that interpolate. In *ACM Transactions on Graphics*, volume 21, pages 855–873, 2002.